Title

PI3Kγ/AKT signaling in high molecular weight hyaluronan (HMWH)-induced anti-hyperalgesia and reversal of nociceptor sensitization

Journal

Journal of Neuroscience, 41(40)

ISSN

0270-6474

Authors

Bonet, Ivan JM
Khomula, Eugen V
Araldi, Dionéia
et al.

Publication Date

2021-10-06

DOI

10.1523/jneurosci.1189-21.2021

Peer reviewed

Behavioral/Cognitive

PI3Kγ/AKT Signaling in High Molecular Weight Hyaluronan (HMWH)-Induced Anti-Hyperalgesia and Reversal of Nociceptor Sensitization

Ivan J. M. Bonet,[1*] Eugen V. Khomula,[1*] Dionéia Araldi,[1] Paul G. Green,[2] and Jon D. Levine[3]

[1]Departments of Oral and Maxillofacial Surgery and, Division of Neuroscience, University of California at San Francisco, San Francisco, California 94143, [2]Departments of Preventative and Restorative Dental Sciences and Oral and Maxillofacial Surgery and Division of Neuroscience, University of California at San Francisco, San Francisco, California 94143, and [3]Departments of Medicine and Oral and Maxillofacial Surgery, Division of Neuroscience and UCSF Pain and Addiction Research Center, University of California at San Francisco, San Francisco, California 94143

High molecular weight hyaluronan (HMWH), a well-established treatment for osteoarthritis pain, is anti-hyperalgesic in preclinical models of inflammatory and neuropathic pain. HMWH-induced anti-hyperalgesia is mediated by its action at cluster of differentiation 44 (CD44), the cognate hyaluronan receptor, which can signal via phosphoinositide 3-kinase (PI3K), a large family of kinases involved in diverse cell functions. We demonstrate that intrathecal administration of an oligodeoxynucleotide (ODN) antisense to mRNA for PI3Kγ (a Class I PI3K isoform) expressed in dorsal root ganglia (DRGs), and intradermal administration of a PI3Kγ-selective inhibitor (AS605240), markedly attenuates HMWH-induced anti-prostaglandin E_2 (PGE_2) hyperalgesia, in male and female rats. Intradermal administration of inhibitors of mammalian target of rapamycin (mTOR; rapamycin) and protein kinase B (AKT; AKT Inhibitor IV), signaling molecules downstream of PI3Kγ, also attenuates HMWH-induced anti-hyperalgesia. *In vitro* patch-clamp electrophysiology experiments on cultured nociceptors from male rats demonstrate that some HMWH-induced changes in generation of action potentials (APs) in nociceptors sensitized by PGE_2 are PI3Kγ dependent (reduction in AP firing rate, increase in latency to first AP and increase in slope of current ramp required to induce AP) and some are PI3Kγ independent [reduction in recovery rate of AP afterhyperpolarization (AHP)]. Our demonstration of a role of PI3Kγ in HMWH-induced anti-hyperalgesia and reversal of nociceptor sensitization opens a novel line of research into molecular targets for the treatment of diverse pain syndromes.

Key words: **anti-hyperalgesia; electrical excitability; high molecular weight hyaluronan; hyperalgesia; phosphoinositide 3-kinases**

Significance Statement

We have previously demonstrated that high molecular weight hyaluronan (HMWH) attenuates inflammatory hyperalgesia, an effect mediated by its action at cluster of differentiation 44 (CD44), the cognate hyaluronan receptor, and activation of its downstream signaling pathway, in nociceptors. In the present study, we demonstrate that phosphoinositide 3-kinase (PI3K) γ and downstream signaling pathway, protein kinase B (AKT) and mammalian target of rapamycin (mTOR), are crucial for HMWH to induce anti-hyperalgesia.

Introduction

Intra-articular administration of high molecule weight hyaluronan (HMWH), an integral component of extracellular matrix (Toole, 2009; Tavianatou et al., 2019), used clinically in the treatment of osteoarthritis pain (Dougados et al., 1993; Altman and Moskowitz, 1998; Cohen et al., 2008; Huang et al., 2011; Triantaffilidou et al., 2013), has anti-inflammatory and immunosuppressant effects (Cuff et al., 2001; Mizrahy et al., 2011; Kataoka et al., 2013; Furuta et al., 2017; Wu et al., 2017). We and others have shown an anti-hyperalgesic effect of HMWH mediated by its action on nociceptor peripheral terminals (Gomis et al., 2007; Caires et al., 2015; de la Peña et al., 2016; Ferrari et al.,

Received June 9, 2021; revised Aug. 9, 2021; accepted Aug. 12, 2021.

Author contributions: I.J.M.B., E.V.K., P.G.G., and J.D.L. designed research; I.J.M.B., E.V.K., and D.A. performed research; I.J.M.B., E.V.K., D.A., and J.D.L. analyzed data; I.J.M.B. wrote the first draft of the paper; J.D.L. edited the paper; I.J.M.B., E.V.K., D.A., and J.D.L. wrote the paper.

This work was supported by the National Institutes of Health Grant AR075334. We thank Niloufar Mansooralavi for technical assistance.

*I.J.M.B. and E.V.K. contributed equally to this work.

The authors declare no competing financial interests.

Correspondence should be addressed to Jon D. Levine at jon.levine@ucsf.edu.

https://doi.org/10.1523/JNEUROSCI.1189-21.2021

2016b, 2018; Bonet et al., 2020b). HMWH, which has average molecular weight between 1.5 and 2 MDa (Gruber et al., 2021), can reduce the activation of transient receptor potential vanilloid subtype 1 (TRPV1) channel by stabilizing its closed state (Caires et al., 2015; de la Peña et al., 2016) also binds to and signals via plasma membrane receptors, including cluster of differentiation 44 (CD44) and Toll-like receptor 4 (TLR4; Vigetti et al., 2014a,b; Ferrari et al., 2018; Tavianatou et al., 2019; Bonet et al., 2020a,b). Attenuation of CD44 and TLR4 on nociceptors, by intrathecal administration of antisense oligodeoxynucleotides (ODNs), or intradermal administration of receptor antagonists, decreases HMWH-induced anti-hyperalgesia (Ferrari et al., 2016b; Bonet et al., 2020b), as does blocking CD44 signaling by two phosphoinositide 3-kinase (PI3K) inhibitors, wortmannin and LY249002 (Bonet et al., 2020b).

PI3K is a family of kinases involved in diverse cellular functions (Rückle et al., 2006; Ali et al., 2008; Morello et al., 2009; Jin et al., 2020). At the plasma membrane, they convert phosphatidyl-inositol biphosphate (PIP2) to phosphatidyl-inositol triphosphate (PIP3) that, in turn, induces downstream signaling events, including activation of protein kinase B (AKT) and mammalian target of rapamycin (mTOR; Engelman et al., 2006; Shaw and Cantley, 2006; Wullschleger et al., 2006). There are several PI3K isoforms in the dorsal root ganglion (DRG; i.e., PI3Kα, PI3Kβ, PI3Kδ, and PI3Kγ; Leinders et al., 2014). The Class I PI3K isoform, PI3Kγ is rapidly activated by G-protein-coupled receptors (GPCRs) to regulate cellular functions such as cell survival, proliferation, migration, and adhesion (Rommel et al., 2007). Expressed in the brain (Eickholt et al., 2007) and DRG (Leinders et al., 2014) PI3Kγ has been implicated in both nociception and anti-nociception (Cunha et al., 2010; Pritchard et al., 2016).

In the current study, we investigated the effect of blocking PI3Kγ, via intrathecal administration of ODN antisense to PI3Kγ mRNA and intradermal administration of a PI3Kγ inhibitor, on the anti-hyperalgesia induced by HMWH, and explored the role of AKT and mTOR signaling, which is downstream of PI3Kγ. Additionally, in cultured DRG neurons, we examined the role of PI3Kγ in electrophysiological correlates of HMWH-induced anti-hyperalgesia, in prostaglandin E_2 (PGE_2) sensitized nociceptors.

Materials and Methods

Animals

Experiments were performed on 220- to 400-g female and male Sprague Dawley rats (Charles River Laboratories). Experimental animals were housed three per cage, under a 12/12 h light/dark cycle, in a temperature-controlled and humidity-controlled animal care facility of the University of California, San Francisco. Food and water were available *ad libitum*. Experimental protocols were approved by the Institutional Animal Care and Use Committee at the University of California, San Francisco, and adhered to the National Institutes of Health *Guidelines for the Care and Use of Laboratory Animals*.

Measuring nociceptive threshold

Mechanical nociceptive threshold was quantified using an Ugo Basile Analgesymeter (Stoelting), to perform the Randall–Selitto paw-withdrawal test (Randall and Selitto, 1957; Taiwo et al., 1989; Taiwo and Levine, 1989). This device applies a linearly increasing mechanical force to the dorsum of the rat's hind paw. Rats were placed in cylindrical acrylic restrainers with lateral ports that allow access to the hind paw (Araldi et al., 2019), for 30 min, to acclimatize them to the testing procedure.

Mechanical nociceptive threshold is defined as the force in grams at which a rat withdraws its hind paw. Baseline threshold is defined as the mean of three readings taken before injection of test agents. Each experiment was performed on a different group of rats. Data are presented as mean change from baseline nociceptive threshold.

Drugs

The following drugs were used in this study: high molecular weight hyaluronan (HMWH; hyaluronic acid sodium salt from Streptococcus pyogenes; molecular weight range 5.0×10^5 to 1.2×10^6 kDa), rapamycin (an mTOR inhibitor) and AKT Inhibitor IV (a protein kinase B inhibitor) from Calbiochem; PGE_2 from Sigma-Aldrich; and AS605240 (a PI3Kγ inhibitor) purchased from Tocris.

PGE_2 was dissolved in absolute ethanol to a concentration of 1 μg/μl, to produce its stock solution, and further diluted in saline, immediately before experiments. The ethanol concentration of the final PGE_2 solution was ~2%, a concentration previously shown to not affect mechanical nociceptive threshold (Ferrari et al., 2016a).

Aliquots of HMWH, dissolved in distilled water to a concentration of 1 μg/μl, were further diluted in saline to the concentration used in each experiment. Aliquots containing 1 μg/μl of AS605240, rapamycin, and AKT Inhibitor IV, dissolved in 100% dimethyl sulfoxide (DMSO), were diluted in 0.9% NaCl containing 1% DMSO to their final concentration.

All drugs administered intradermally were in a volume of 5 μl (when one drug was injected) or 3 μl each (when two or more drugs were injected), on the dorsum of the hind paw, using a 30-gauge hypodermic needle attached to a 50-μl Hamilton syringe by PE-10 polyethylene tubing (Becton Dickinson). The administration of AS605240, rapamycin and AKT Inhibitor IV was preceded by 1 μl of distilled water, separated by an air bubble, to avoid mixing, to produce hypotonic shock, transiently enhancing cell permeability, facilitating penetration of reagents into the terminals (Borle and Snowdowne, 1982; Burch and Axelrod, 1987).

ODN antisense to PI3Kγ mRNA

The role of PI3Kγ in the anti-nociceptive effect of HMWH was assessed in male and female rats treated intrathecally with ODN antisense against a unique region of the rat PI3Kγ mRNA sequence for.

Antisense ODN sequence

PI3Kγ ODN antisense: 5′-AAA AGT TGC AGT CCA GGA GTT-3′ (GenBank accession number NM_133399.3).

Mismatch ODN sequence, corresponding to the antisense sequence with mismatched bases (denoted by bold letters), had no sequence homology in the rat gene database.

Mismatch ODN sequences

PI3Kγ ODN mismatch: 5′-AAA **C**GT **A**GC A**T**T CC**T** **C**GA G**A**T-3′

This ODN antisense sequence, synthesized by Life Technologies, has been previously shown to produce a decrease in PI3Kγ in rat DRG (Cunha et al., 2010). Before use, ODNs are reconstituted in nuclease-free 0.9% NaCl and then administered intrathecally. As described previously (Alessandri-Haber et al., 2003), rats were anesthetized with isoflurane (2.5% in O_2) and 120 μg of ODN, in a volume of 20 μl, injected intrathecally using an insulin syringe (300 units/μl) attached to a 29-gauge needle inserted into the subarachnoid space between the L4 and L5 vertebrae. The intrathecal site of injection was confirmed by a flick of the rat's tail, a reflex that is evoked by subarachnoid space access and bolus intrathecal injection (Mestre et al., 1994). Animals regained consciousness ~2 min after injections. The use of antisense ODN administered intrathecally, to attenuate the expression of proteins essential for their role in nociceptor sensitization, is well supported by previous studies by others (Song et al., 2009; Su et al., 2011; Quanhong et al., 2012; Sun et al., 2013; Oliveira-Fusaro et al., 2017), as well as our group (Parada et al., 2003; Bogen et al., 2012; Alvarez et al., 2014; Ferrari et al., 2016a,b, 2018; Araldi et al., 2017, 2019).

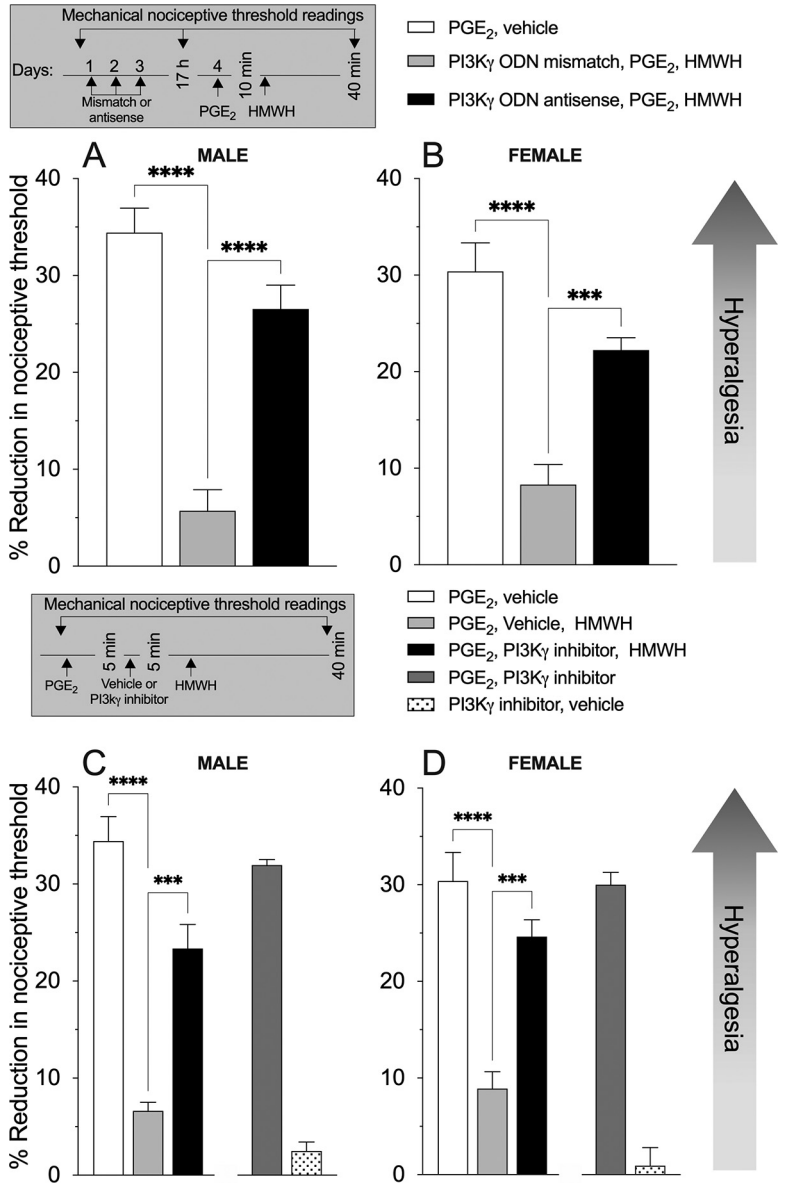

Figure 1. Reversal of PGE_2 hyperalgesia by HMWH is attenuated by ODN antisense to PI3K γ mRNA and a PI3K γ inhibitor. ***A***, ***B***, Male and female rats were treated intrathecally (i.t.) with an ODN antisense or mismatch (120 μg/20 μl, i.t.) for PI3K γ mRNA, daily for three consecutive days. On the fourth day, ~17 h after the last i.t. administration of ODN, PGE_2 (100 ng/5 μl, i.d.) was injected intradermally (i.d.) on the dorsum of the hind paw, followed 10 min later by HMWH (1 μg/5 μl, i.d.) or vehicle (5 μl, i.d.). Mechanical nociceptive threshold was evaluated before and 40 min after i.d. PGE_2. HMWH attenuates PGE_2-induced hyperalgesia (***A***, $F_{(2,15)} = 38.46$, $^{****}p < 0.0001$, when PGE_2 was compared with PGE_2 + HMWH-treated group; one-way ANOVA followed by Bonferroni's *post hoc* comparisons test), and the anti-hyperalgesic effect of HMWH on PGE_2-induced hyperalgesia is attenuated by PI3K γ antisense ODN, in male rats ($^{****}p < 0.0001$, when HMWH-induced anti-hyperalgesia was compared between PI3K γ mismatch-treated and PI3K γ antisense-treated groups at 40 min after PGE_2; one-way ANOVA followed by Bonferroni's *post hoc* comparisons test). In female rats, i.d. HMWH also attenuates PGE_2-induced hyperalgesia (***B***, $F_{(2,15)} = 25.41$, $^{****}p < 0.0001$, when PGE_2 was compared with PGE_2 + HMWH-treated group; one-way ANOVA followed by Bonferroni's *post hoc* comparisons test). And treatment with PI3K γ antisense ODN also attenuates HMWH-induced anti-hyperalgesia ($^{***}p = 0.0009$, when HMWH-induced anti-hyperalgesia was compared between PI3K γ mismatch-treated and PI3K γ antisense-treated groups measured 40 min after PGE_2; one-way ANOVA followed by Bonferroni's *post hoc* comparisons test); $n = 6$ each group. ***C***, ***D***, Male and female rats were treated with PGE_2 (100 ng/3 μl, i.d.) followed 5 min later by a PI3K γ inhibitor (AS605240, 1 μg/3 μl, i.d.) or vehicle (3 μl, i.d.); 10 min after injection of PGE_2, rats received an injection of HMWH (1 μg/3 μl, i.d.); mechanical nociceptive threshold was evaluated before and 40 min after i.d. PGE_2. Additional groups of male and female rats only received the PI3K γ inhibitor (1 μg/3 μl, i.d.), to confirm that it did not alone produce hyperalgesia, and another group of rats received PGE_2 (100 ng/3 μl, i.d.), followed 5 min later by the PI3K γ inhibitor (1 μg/3 μl, i.d.) to show that PI3K γ inhibitor did not alone affect PGE_2-induced hyperalgesia (dotted and dark gray bars, respectively). Intradermal HMWH attenuates PGE_2-induced hyperalgesia (***C***, $F_{(2,15)} = 44.00$, $^{****}p < 0.0001$; ***D***, $F_{(2,15)} = 24.98$, $^{****}p < 0.0001$, when PGE_2- was compared with PGE_2 + HMWH-treated group; one-way ANOVA followed by Bonferroni's *post hoc* comparisons test). The anti-hyperalgesic effect of HMWH was attenuated by the PI3K γ inhibitor, in male and female rats (***C***, $^{***}p = 0.0001$; ***D***, $^{***}p = 0.0003$, when HMWH-induced anti-hyperalgesia was compared between vehicle-treated and PI3K γ inhibitor-treated groups at 40 min after PGE_2 in male and female rats, respectively; one-way ANOVA followed by Bonferroni's *post hoc* comparisons test); $n = 6$ each group.

Culture of DRG neurons

Primary neuronal cultures were made from dissociated DRGs harvested from adult male Sprague Dawley rats (300–400 g), as described previously (Khomula et al., 2021). In brief, under isoflurane anesthesia, rats were decapitated and the dorsum of the vertebral column surgically removed; L_4 and L_5 DRGs were rapidly extracted, bilaterally, chilled and desheathed in HBSS, on ice. Ganglia were then treated with 0.25% collagenase type 4 (Worthington Biochemical Corporation) in HBSS for 18 min at 37°C, and followed by treatment with 0.25% trypsin (Worthington Biochemical Corporation) in calcium-free and magnesium-free PBS (Invitrogen Life Technologies) for 6 min, followed by three washes, and then trituration in Neurobasal-A medium (Invitrogen Life Technologies), to produce a single-cell suspension. This cell suspension was centrifuged at 1000 RPM for 3 min and re-suspended in Neurobasal-A medium supplemented with 50 ng/ml nerve growth factor, 100 U/ml penicillin/streptomycin, B-27, GlutaMAX, and 10% fetal bovine serum (Invitrogen Life Technologies). Cells were then plated on cover slips and incubated at 37°C in 3.5% CO_2 for at least 24 h before use in experiments.

In vitro patch-clamp electrophysiology

DRG neurons were used in electrophysiology experiments 24–96 h after plating. DRGs from at least three rats (separate culture preparations) were used for each experimental series. Within the text, *n* refers to number of neurons. Cells were identified as neurons by their double birefringent plasma membranes (Cohen et al., 1968; Landowne, 1993). While small, medium and large sized DRG neurons were routinely observed in the same preparation, this study focused on cells with soma diameter <30 μm (small DRG neurons), predominantly representing C-type nociceptors (Harper and Lawson, 1985; Gold et al., 1996; Petruska et al., 2000, 2002; Woolf and Ma, 2007). After mounting a coverslip plated with cells in the recording chamber, the culture medium was replaced with Tyrode's solution containing 140 mM NaCl, 4 mM KCl, 2 mM $MgCl_2$, 2 mM $CaCl_2$, 10 mM glucose, 10 mM HEPES, and adjusted to pH 7.4 with NaOH; osmolarity is 310 mOsm/kg (Ferrari et al., 2018; Khomula et al., 2019, 2021). Tyrode's solution was used as external perfusion solution. Drugs used *in vitro* were diluted to their final concentration in this solution, just before application. The volume of the recording chamber is 150 μl. The perfusion system is gravity-driven, flow rate of 0.5–1 ml/min. All experiments were performed at room temperature (20–23°C).

Whole-cell patch-clamp recordings, in current clamp mode, were made to assess changes in the excitability of cultured DRG neurons.

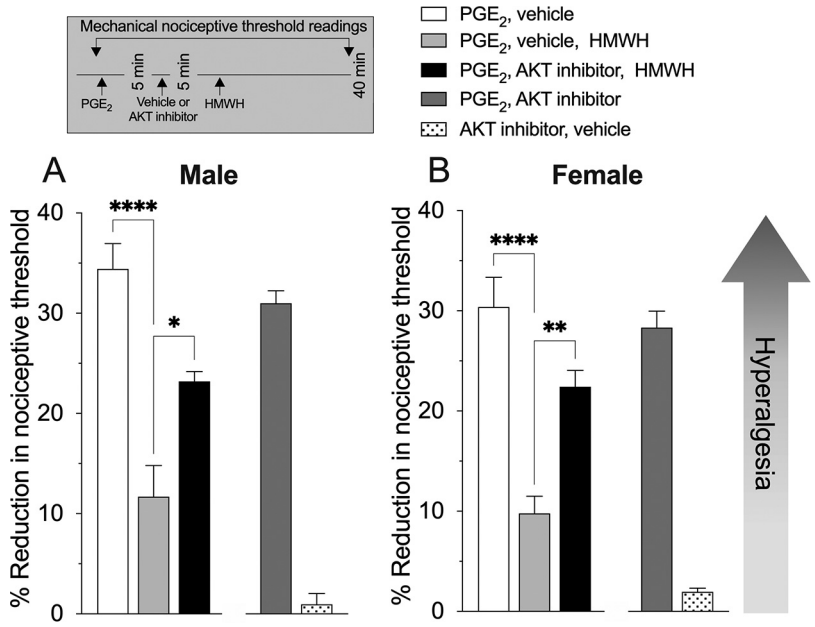

Figure 2. HMWH-induced anti-hyperalgesia is protein kinase B (AKT) dependent. Male and female rats were treated intradermally with PGE_2 (100 ng/3 µl, i.d.) followed 5 min later by an AKT inhibitor (AKT Inhibitor IV, 1 µg/3 µl, i.d.) or vehicle (3 µl, i.d.); 10 min after PGE_2, rats received HMWH (1 µg/3 µl, i.d.) and mechanical nociceptive threshold evaluated 40 min after PGE_2. Additional groups of male and female rats received the AKT inhibitor (1 µg/3 µl, i.d.) alone, to confirm that it did not produce hyperalgesia. Additional groups of male and female rats received PGE_2 (100 ng/3 µl, i.d.) followed 5 min later by the AKT inhibitor (1 µg/3 µl, i.d.), to determine whether the AKT inhibitor alone did not affect PGE_2-induced hyperalgesia (dotted and dark gray bars, respectively). ***A***, Male: PGE_2-induced hyperalgesia is attenuated by intradermal HMWH ($F_{(2,15)} = 22.67$, $^{****}p < 0.0001$, when PGE_2- was compared with PGE_2 + HMWH-treated group; one-way ANOVA followed by Bonferroni's *post hoc* comparisons test). Treatment with the AKT inhibitor attenuates HMWH-induced anti-hyperalgesia in male rats ($^{*}p = 0.0125$, when HMWH-induced anti-hyperalgesia was compared between vehicle-treated and AKT Inhibitor IV-treated groups at 40 min after PGE_2; one-way ANOVA followed by Bonferroni's *post hoc* comparisons test); $n = 6$ each group. ***B***, Female: intradermal HMWH attenuates PGE_2-induced hyperalgesia in female rats ($F_{(2,15)} = 22.59$, $^{****}p < 0.0001$, when PGE_2- was compared with PGE_2 + HMWH-treated group; one-way ANOVA followed by Bonferroni's *post hoc* comparisons test). Treatment with the AKT inhibitor also attenuates HMWH-induced anti-hyperalgesia ($^{**}p = 0.0019$, when HMWH-induced anti-hyperalgesia was compared between vehicle-treated and AKT Inhibitor IV-treated groups at 40 min after PGE_2; one-way ANOVA followed by Bonferroni's *post hoc* comparisons test); $n = 6$ each group.

Holding current was adjusted to maintain membrane potential at −70 mV. Rheobase, the minimum magnitude of a current step needed to elicit an action potential (AP), was determined using a protocol where increasing square wave (40–80 ms) current pulses were applied every 2 s with step adjusted with 5–10% precision (Ferrari et al., 2018; Khomula et al., 2019, 2021).

Number of APs was counted during a 250-ms current step stimulation above rheobase. Average firing frequency was defined as number of intervals between APs (i.e., number of APs minus one) divided by time between first and last AP during that stimulation.

AP threshold potential was determined from an approximation of the initial phase of the response to a square wave current pulse of rheobase magnitude with sum of decaying and rising exponents, representing membrane capacitance recharge and initial rising phase of AP development (Duzhyy et al., 2015; Viatchenko-Karpinski and Gu, 2016; Ferrari et al., 2018). AP threshold was defined as the potential on the recording where the difference from the decaying component of the fit raised above the arbitrary selected value of 2 mV, representing sensitivity of the definition. In ramp protocol, the linear part preceding first AP was fitted with a straight line. Similarly, AP threshold was defined as the point where deviation from the fitted straight line exceeded 2 mV.

The following electrophysiological properties describing afterhyperpolarization (AHP) phase of AP were assessed in APs evoked by a short (1–3 ms) depolarizing current pulse: magnitude (defined as distance from AHP minimum to the baseline membrane potential) and time constant of recovery to baseline (defined from the fit with a single exponential function; Ferrari et al., 2018).

Latency to the peak of the first AP was measured using a protocol consisting of ramp current pulse with duration from 200 to 500 ms and slope factor from 0.2 to 4 pA/ms (Ferrari et al., 2018).

Recording electrodes were fabricated from borosilicate glass capillaries (0.84/1.5 mm i.d./o.d., Warner Instruments, LLC) using a Flaming/Brown P-87 puller (Sutter Instrument Co). Recording electrode resistance was ~3 MΩ after being filled with a solution containing the following: 130 mM KCl, 10 mM HEPES, 10 mM EGTA, 1 mM $CaCl_2$, 5 mM MgATP, and 1 mM Na-GTP, pH 7.2 (adjusted with Tris-base), 300 mOsm (measured by Wescor Vapro 5520 osmometer, ELITech Group; Ferrari et al., 2018; Khomula et al., 2021). Junction potential was not adjusted. Series resistance was below 20 MΩ at the end of recordings and was not compensated. Recordings were made with an Axon MultiClamp 700 B amplifier, filtered at 10 kHz, and sampled at 20 kHz using Axon Digidata 1550B controlled by pCLAMP 11 software (all from Molecular Devices LLC).

Drugs were applied at least 10 min after the establishment of whole-cell configuration, at which time baseline current was stable. To parallel *in vivo* experiments, *in vitro* experiments were also performed using a reversal protocol, where PGE_2 (1 µM) was applied first, to induce sensitization, and 10 min later, HMWH (0.2 g/l) was applied to examine its effects on sensitized neurons. In experiments exploring the effect of PI3Kγ inhibition, a selective PI3Kγ inhibitor, AS605240 (1 µM) was co-administered with PGE_2 and remained present during recordings. For the parameters where a significant effect of HMWH was established, the effect of HMWH alone was additionally examined, in a separate group of neurons.

Statistical analysis

In behavioral experiments, the dependent variable was percentage change from baseline mechanical nociceptive paw-withdrawal threshold. We used 186 male and 96 female rats in the behavioral experiments. In each experiment only one hind paw per rat was used. The behavioral experiments were performed with the experimenter blinded to experimental group. Repeated-measures one-way ANOVA followed by Bonferroni's *post hoc* multiple comparisons test or Student's *t* test was used to analyze data.

In *in vitro* experiments, electrophysiological parameters were measured before and 10 min after application of PGE_2 (just before application of HMWH) and then 10 min after application of HMWH, to assess the effect produced by HMWH. Magnitude of the effect of a drug was expressed as percentage change in a parameter, i.e., value before drug administration was subtracted from value after, then the difference was divided by a baseline, which was set to a value of the parameter recorded after PGE_2 administration (for PGE_2, and HMWH after PGE_2) or a pre-administration value (for HMWH alone), then the ratio was multiplied by 100%. Only neurons in which reduction in rheobase was >10%, 10 min after PGE_2, were considered PGE_2 responsive and included in our analysis. As outlined in the corresponding figure legends, the following statistical tests were used: paired and unpaired two-tailed Student's *t* test, one-sample two-tailed Student's *t* test versus zero, one-way ANOVA with followed by Dunnett's *post hoc* test .

Prism 8.0 (GraphPad Software) was used for the graphics and to perform statistical analyses; $p < 0.05$ was considered statistically significant. Data are presented as mean ± SEM.

Results

HMWH-induced anti-hyperalgesia is PI3Kγ dependent

We have previously shown that PI3K, downstream of CD44, is involved in HMWH-induced anti-hyperalgesia (Bonet et al., 2020b). In the present experiments we tested the hypothesis that HMWH anti-hyperalgesia is PI3Kγ dependent. Male (Fig. 1*A*) and female (Fig. 1*B*) rats received intrathecal injections of ODN antisense to PI3Kγ mRNA on three consecutive days. On the fourth day, ~17 h after the last ODN administration, PGE_2 was injected intradermally (100 ng, i.d.), on the dorsum of the hind paw, followed 10 min later by HMWH (1 µg, i.d.), at the same site. Attenuation of HMWH-induced anti-hyperalgesia was observed in both male and female rats that received PI3Kγ ODN antisense (Fig. 1*A*, $F_{(2,15)} = 38.46$, $^{****}p < 0.0001$; Fig. 1*B*, $F_{(2,15)} = 25.41$, $^{***}p = 0.0009$).

Additional groups of male and female rats received an intradermal injection of PGE_2 (100 ng, i.d.) followed by a PI3Kγ inhibitor (AS605240, 3 µg, i.d.), and then, 5 min later, HMWH (1 µg, i.d.), all injected at the site of nociceptor testing. Male (Fig. 1*C*) and female (Fig. 1*D*) rats receiving the PI3Kγ inhibitor showed attenuation of HMWH-induced anti-hyperalgesia of similar magnitude to that produced by PI3Kγ ODN antisense (Fig. 1*C*, $F_{(2,15)} = 44.00$, $^{***}p = 0.0001$; Fig. 1*D*, $F_{(2,15)} = 24.98$, $^{***}p = 0.0003$).

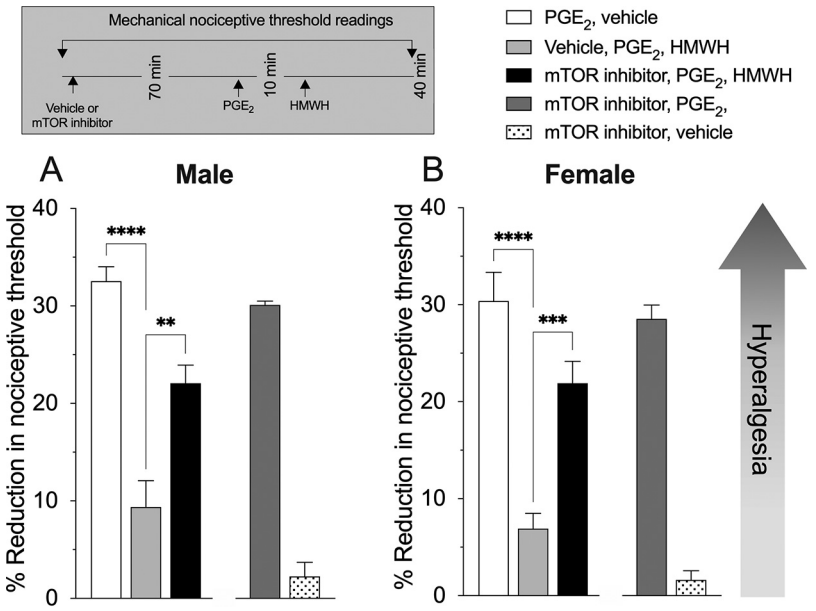

Figure 3. HMWH-induced anti-hyperalgesia is mTOR dependent. Male and female rats were treated intradermally with a mTOR inhibitor (rapamycin, 1 µg/3 µl, i.d.) or vehicle (3 µl, i.d.). Seventy minutes later, rats received PGE_2 (100 ng/3 µl, i.d.) followed 10 min later by HMWH (1 µg/3 µl, i.d.), and mechanical nociceptive threshold evaluated 40 min after PGE_2. Additional groups of male and female rats received mTOR inhibitor (1 µg/3 µl, i.d.) to confirm that it did not itself produce hyperalgesia. Additional groups of male and female rats received PGE_2 (100 ng/3 µl, i.d.) followed 5 min later by the mTOR inhibitor (1 µg/3 µl, i.d.), to show that the mTOR inhibitor did not alone affect PGE_2-induced hyperalgesia (dotted and dark gray bars, respectively). ***A***, Male: HMWH attenuates PGE_2-induced hyperalgesia in male rats ($F_{(2,15)} = 30.97$, $^{****}p < 0.0001$, when the PGE_2 group was compared with PGE_2 + HMWH-treated group; one-way ANOVA followed by Bonferroni's *post hoc* comparisons test). Pretreatment with the mTOR inhibitor attenuates HMWH-induced anti-hyperalgesia ($^{**}p = 0.0012$, when HMWH-induced anti-hyperalgesia was compared between vehicle-treated and mTOR inhibitor-treated groups at 40 min after PGE_2; one-way ANOVA followed by Bonferroni's *post hoc* comparisons test); $n = 6$ each group. ***B***, Female: intradermal HMWH attenuates PGE_2-induced hyperalgesia in female rats ($F_{(2,15)} = 25.90$, $^{****}p < 0.0001$, when PGE_2-treated was compared with PGE_2 + HMWH-treated group; one-way ANOVA followed by Bonferroni's *post hoc* comparisons test). Female rats that received pretreatment of the mTOR inhibitor also show attenuation of HMWH-induced anti-hyperalgesia ($^{***}p = 0.0008$, when HMWH-induced anti-hyperalgesia was compared between vehicle-treated and mTOR Inhibitor IV-treated groups at 40 min after PGE_2; one-way ANOVA followed by Bonferroni's *post hoc* comparisons test); $n = 6$ each group.

Role of AKT/mTOR

Since AKT and mTOR can signal downstream of PI3K (Franke et al., 2003; Cunha et al., 2010), we next evaluated their role in HMWH-induced anti-hyperalgesia. To test the hypothesis that HMWH signals through AKT, to induce anti-hyperalgesia, male (Fig. 2*A*) and female (Fig. 2*B*) rats were treated intradermally with PGE_2 (100 ng, i.d.), followed 5 min later by an AKT inhibitor (AKT Inhibitor IV, 1 µg, i.d.) and then a further 5 min later by HMWH (1 µg, i.d.), all at the site of nociceptive testing on the dorsum of the hind paw. Rats treated with the AKT inhibitor showed attenuation of HMWH-induced anti-hyperalgesia (Fig. 2*A*, $F_{(2,15)} = 22.67$, $^{*}p < 0.0125$; Fig. 2*B*, $F_{(2,15)} = 22.59$, $^{**}p < 0.0019$).

To determine whether HMWH-induced anti-hyperalgesia is also mTOR-dependent, male (Fig. 3*A*) and female (Fig. 3*B*) rats were treated intradermally with an mTOR inhibitor (rapamycin, 1 µg, i.d.) followed 70 min later by PGE_2 (100 ng, i.d.) and then a further 10 min later by HMWH (1 µg, i.d.). Rats pretreated with the mTOR inhibitor showed attenuation of HMWH-induced anti-hyperalgesia (Fig. 3*A*, $F_{(2,15)} = 30.97$, $^{**}p = 0.0012$; Fig. 3*B*, $F_{(2,15)} = 25.90$, $^{***}p = 0.0008$).

HMWH attenuates nociceptor sensitization, *in vitro*

The results of our behavioral experiments support the suggestion that HMWH-induced anti-hyperalgesia is PI3Kγ dependent, in both male and female rats, without sex differences (Fig. 1). Since the behavioral experiments did not show differences between males and females, in our *in vitro* electrophysiology experiments, we used DRG neurons from male rats. To elucidate electrophysiological mechanisms of HMWH-induced anti-hyperalgesia, at the level of the nociceptor, we performed *in vitro* experiments on cultured DRG neurons and examined the effect of HMWH on parameters describing electrical excitability, in nociceptors. To parallel *in vivo* experiments, *in vitro* experiments were also performed using a reversal protocol, where PGE_2 (1 µM) was applied first, to induce sensitization, and 10 min later, HMWH (0.2 g/L) was applied, to examine its effects on sensitized neurons (for schematic of the protocol, see Fig. 4*A*, inset).

We first tested whether HMWH attenuates changes in frequency and number of APs in neurons sensitized by PGE_2 and whether such attenuation was PI3Kγ dependent. Out of 11 small-diameter DRG neurons, in which sensitization by PGE_2 (1 µM) was confirmed by an at least 10% reduction of AP

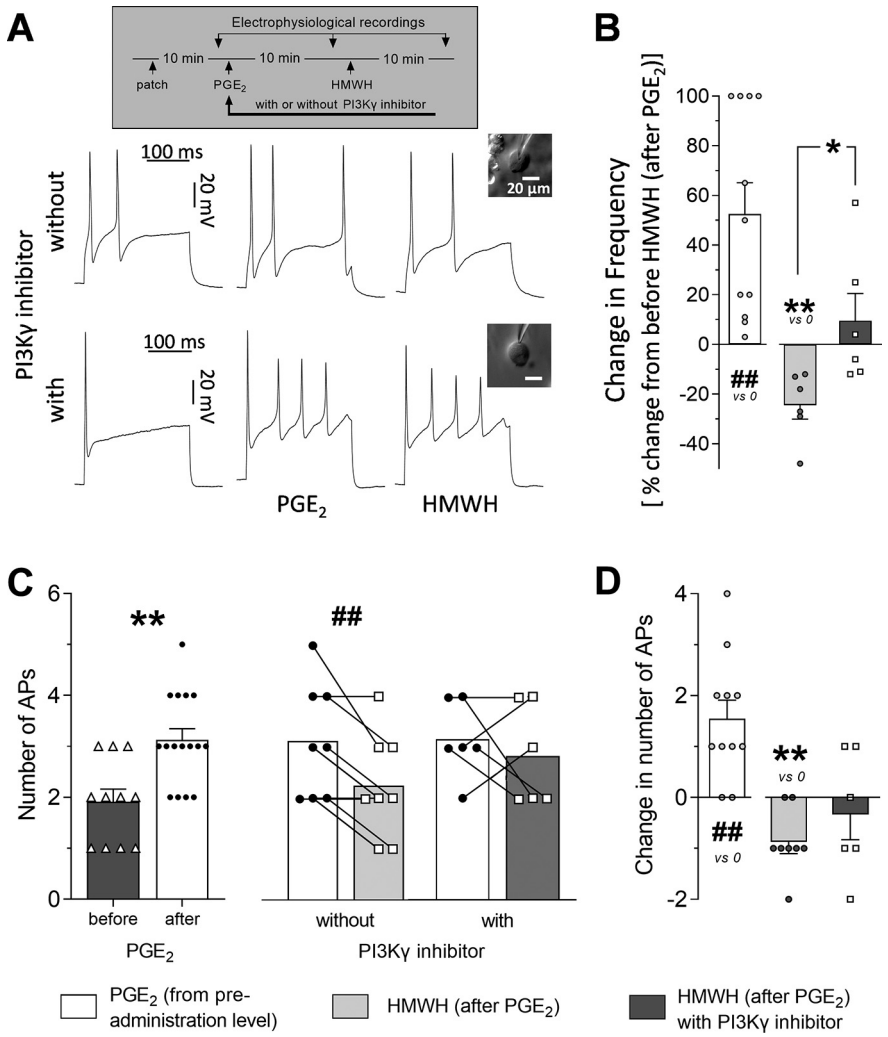

Figure 4. PI3K γ inhibitor prevents attenuating effect of HMWH on enhanced activity in nociceptors sensitized by PGE_2. ***A***, Firing of two small DRG neurons before PGE_2-induced sensitization (left traces), after sensitization by PGE_2 (1 μM; middle traces), and then after application of HMWH (0.2 g/l; right traces). Electrophysiological traces recorded in current clamp mode of whole-cell patch-clamped neurons show membrane potential. Traces from the same row correspond to the same neuron, depicted in the inset image to the right of recordings (transmitted light, DIC contrast). Neurons were held at −70 mV and stimulated with a current step (250 ms) of the same suprathreshold magnitude in all recordings for the same neuron (usually ~2 times preadministration rheobase was able to generate multiple APs after sensitization). Gray inset above recordings shows timeline of drug administration and activity recordings. In the recordings for the neuron depicted in the bottom set of panels the selective PI3K γ inhibitor AS605240 (1 μM) was administered along with PGE_2 and was present during recordings (middle and right traces). Note the attenuating effect of HMWH on firing activity (top row) and lack of attenuation in the presence of PI3K γ inhibitor (bottom row). ***B***, left panel, Effect of PGE_2 on AP firing frequency, measured as change from preadministration value and expressed as a percentage of the value in the sensitized state (after PGE_2), which is also the value before HMWH. PGE_2 induced a statistically significant increase in firing frequency (one-sample two-tailed Student's *t* test for zero effect: $t_{(10)} = 4.18$, $^{\#\#}p = 0.002$, number of cells is 11). Right panel, Effect of HMWH on AP firing frequency, presented as its relative change from the value before HMWH (in the sensitized state, after PGE_2). HMWH-induced reduction in firing frequency was statistically significant, but not in the presence of PI3K γ inhibitor (one-sample two-tailed Student's *t* test for zero effect: $t_{(5)} = 4.45$, $^{**}p = 0.007$ without the inhibitor and $t_{(5)} = 0.86$, $p = 0.43$ with the inhibitor; $t_{(10)} = 2.76$, $^{*}p = 0.02$, when two groups ware compared with unpaired two-tailed Student's *t* test). Number of cells: six without PI3K γ inhibitor, six with the inhibitor. ***C***, ***D***, Effect of PGE_2 (left panel) and HMWH (right panel) on number of APs. Absolute numbers of APs before and after administration of PGE_2 and then HMWH are shown in ***C***, and their changes ("after" minus "before" for the same neuron) are shown in ***D***. PGE_2-induced an increase in number of APs (left panels in ***C***, ***D***) that is statistically significant (in ***C***, values before and after PGE_2 are compared by unpaired two-tailed Student's *t* test: $t_{(25)} = 3.59$, $^{**}p = 0.0014$, number of cells in: 11 before and 16 after PGE_2; in ***D***, pairwise changes are compared with one-sample two-tailed Student's *t* test for zero effect: $t_{(10)} = 4.22$, $^{\#\#}p = 0.002$, number of cells is 11). Of note, four cells with 100% increase in frequency in ***B*** are those four cells in ***C*** that fired one AP before and two APs after PGE_2. HMWH-induced reduction in number of APs (right panel) was statistically significant, in the absence but not in the presence of PI3K γ inhibitor (when values before and after HMWH were compared by paired two-tailed Student's *t* test: $t_{(7)} = 3.86$, $^{\#\#}p = 0.006$ without inhibitor and $t_{(5)} = 0.67$, $p = 0.53$ with inhibitor). Number of cells in ***C***, ***D***, for the effect of HMWH (right panel): eight without and six with the inhibitor.

rheobase from baseline value (Khomula et al., 2021), six neurons generated multiple (3.2 ± 0.5) APs during a 250-ms current step stimulation, with average frequency of 15 ± 2 Hz. PGE_2 produced a significant increase in both frequency (Fig. 4*A*,*B*, $t_{(10)} = 4.2$, $p = 0.002$) and number of APs (Fig. 4*A*,*C*, $t_{(25)} = 3.6$, $p = 0.0014$; Fig. 4*D*, $t_{(10)} = 4.2$, $p = 0.002$), compared with excitability before PGE_2 sensitization. Then, 10 min after application of HMWH (0.2 g/l) both frequency (Fig. 4*A*,*B*) and number of APs were attenuated (Fig. 4*A*,*C*,*D*). The attenuating effect of HMWH was, however, no longer significant in the presence of the selective PI3K γ inhibitor (AS605240, 1 μM; Fig. 4*B*, $t_{(5)} = 0.9$, $p = 0.4$; Fig. 4*A*,*D*, $t_{(5)} = 0.7$, $p = 0.5$).

Next, we examined whether the attenuating effect of HMWH on hyperexcitability was because of a suppression of PGE_2-induced changes, including its prominent reduction in rheobase and AP onset latency in response to current ramp stimulation, and lowering of AP threshold potential to a more negative value, which is due in part to a potentiating effect of PGE_2 on sodium channels (England et al., 1996; Gold et al., 1998; Ferrari et al., 2018). HMWH-induced changes in these parameters could contribute to the observed decrease in firing rate and number of APs (Fig. 4). As expected, PGE_2 produced robust reduction in rheobase (Fig. 5*A*,*B*, $t_{(23)} = 10.5$, $p < 0.0001$). HMWH did not, however, produce a significant reversal when applied to sensitized nociceptors (Fig. 5*B*, 95% CI of the effect of HMWH is from −4% to +11%; $t_{(13)} = 1.0$, $p = 0.3$). PGE_2 reduced AP threshold potential, by 4 ± 1 mV ($n = 16$, $t_{(15)} = 3.0$, $p = 0.008$), and again HMWH did not produce a significant reversal effect (corresponding change was 0 ± 1 mV; $n = 10$, $t_{(9)} = 0.05$, $p = 0.96$). In agreement with HMWH inducing inhibition of sodium current, we observed a decrease of AP peak potential, by 3 ± 1 mV ($n = 9$, $t_{(8)} = 2.32$, $p = 0.049$). However, this effect of HMWH on AP peak potential was not reversed by PI3K γ inhibitor (AS605240, value of decrease was 7 ± 1 mV; $n = 5$, $t_{(4)} = 5.5$, $p = 0.005$).

Another established method to quantify neuronal excitability is to measure AP onset latency in response to current ramp stimulation (Ferrari et al., 2018; Sun, 2021), where the latency to first AP defines the current

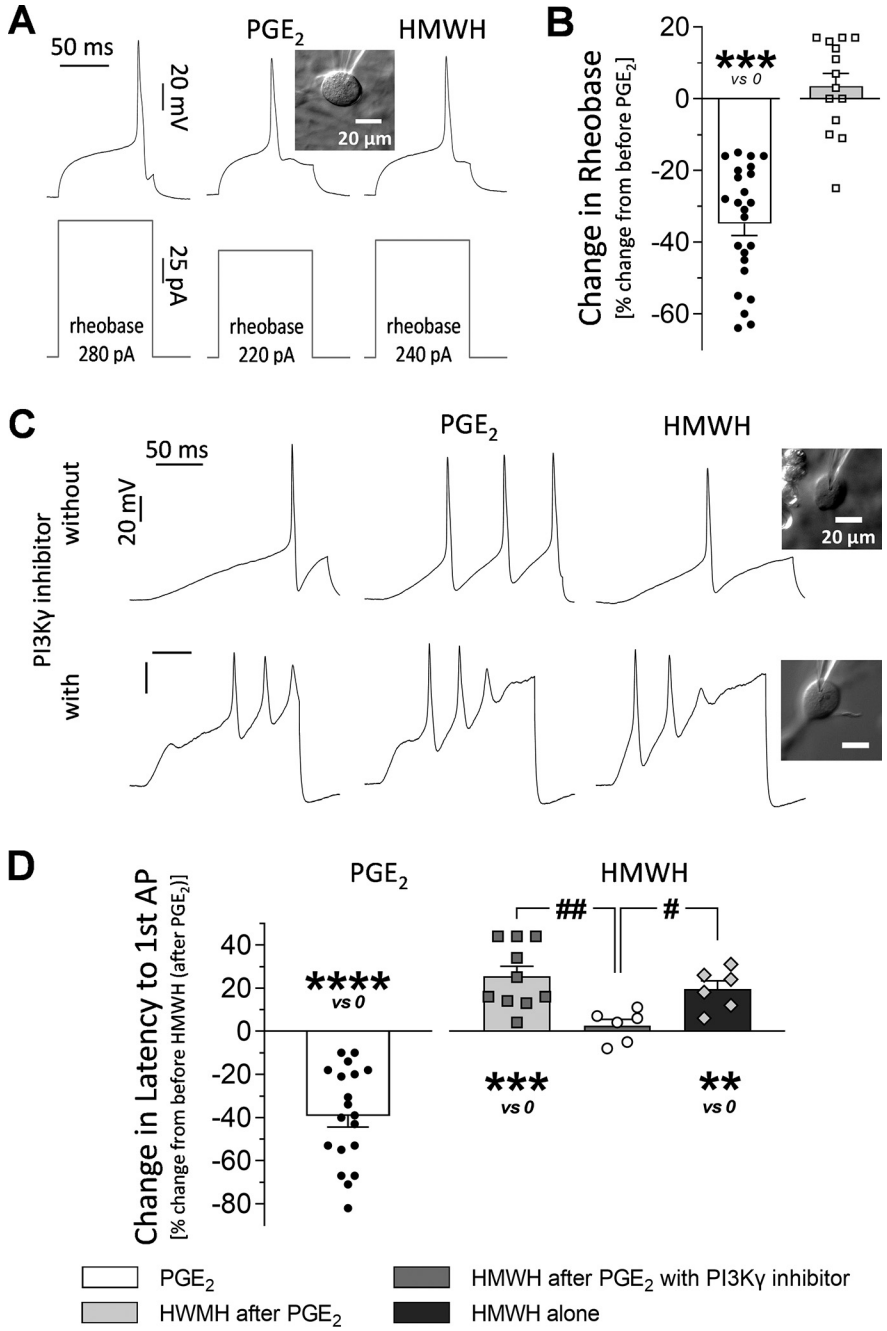

Figure 5. HMWH reverses PGE_2-induced reduction in latency to first AP, but not rheobase, of sensitized nociceptors. ***A***, Example of the lack of effect of HMWH on rheobase (right traces) of a small DRG neuron (depicted in the inset image) after PGE_2 produced significant reduction in rheobase (middle traces), compared with its value before sensitization (left traces). Upper traces show APs generated in response to a current step (depicted below AP recordings) with height equal to rheobase (minimum current required to induce AP, value is indicated). Scale is the same for all traces. Note reduction of current step after PGE_2 with much less change after HMWH. ***B***, Effect of PGE_2 and HMWH (after PGE_2) on AP rheobase. While PGE_2 produced significant reduction in rheobase (one-sample two-tailed Student's *t* test for zero effect: $t_{(23)} = 10.5$, $^{***}p < 0.001$), HMWH administered after PGE_2 did not produce statistically significant reversal (one-sample two-tailed Student's *t* test for zero effect: $t_{(13)} = 1.03$, $p = 0.32$), suggesting lack of reversal of PGE_2-induced changes in rheobase by HMWH. Number of cells: 24 for PGE_2, 14 for HMWH. ***C***, Example of effect of HMWH on latency to first AP (in ramp protocol; right trace) after PGE_2-induced significant reduction in latency (middle trace), compared with its initial value, before sensitization (left trace). Electrophysiological traces show APs generated in two small DRG neurons (depicted in the inset images to the right), one without (upper traces) and one with (bottom traces) PI3Kγ inhibitor, in response to 200-ms stimulation with current ramp (1.5 pA/ms for upper neuron and 7.5 pA/ms for bottom neuron). Scale is the same among traces in the same row. Note the HMWH-induced shift (right trace) of AP toward its initial position (left trace) after the leftward shift produced by PGE_2 (middle trace) and lack of HMWH-induced rightward shift in the presence of the selective PI3Kγ inhibitor AS605240 (1 μM; bottom traces). ***D***, Effect of PGE_2 (left panel) and HMWH [alone and after PGE_2, with and without selective PI3Kγ inhibitor AS605240 (1 μM); right panel] on latency to the first AP in ramp protocol. PGE_2 produced significant reduction in the latency to the first AP (one-sample two-tailed Student's *t* test for zero effect: $t_{(18)} = 7.62$, $^{****}p < 0.001$), while HMWH administered after PGE_2 produced a statistically significant increase (i.e., reversal; one-sample two-tailed Student's *t* test for zero effect: $t_{(9)} = 5.35$, $^{***}p = 0.0005$). There was a statistically significant attenuation of the effect of HMWH (after PGE_2) in the presence of the PI3Kγ inhibitor (one-way ANOVA: $F_{(2,19)} = 6.93$, $p = 0.006$; Dunnett's *post hoc* test: $q_{(19)} = 3.69$, $^{\#\#}$ adjusted $p = 0.003$ with PI3Kγ inhibitor, when compared with HMWH after PGE_2; one-sample two-tailed Student's *t* test for zero effect: $t_{(5)} = 1.79$, $p = 0.13$ with PI3Kγ inhibitor), supporting the suggestion that the effect of HMWH on latency depends on activation of PI3Kγ. The effect of HMWH alone (i.e., without prior sensitization by PGE_2) is also significant (Dunnett's *post hoc* test: $q_{(19)} = 2.45$, $^{\#}$ adjusted $p = 0.043$ for HMWH alone, when compared with HMWH after PGE_2 with PI3Kγ inhibitor; one-sample two-tailed Student's *t* test for zero effect for HMWH alone: $t_{(5)} = 5.12$, $^{**}p = 0.004$), supporting the suggestion that the effect of HMWH on latency does not depend on sensitization. Number of cells: 19 for PGE_2, 10 for HMWH after PGE_2, 6 for HMWH after PGE_2 with PI3Kγ inhibitor, and 6 for HMWH alone. Of note, the value before HMWH is used as a baseline to calculate the effect of HMWH in all cases, regardless of administration of PGE_2, whereas in the case of prior sensitization by PGE_2, "before HMWH" indicates the same value as "after PGE_2" and is also used to calculate % change produced by PGE_2. The same applies to Figure 6*B*,*D*.

threshold to initiate an AP (Fig. 5*C*). PGE_2 produced a significant reduction in AP onset latency (Fig. 5*D*, left panel, $t_{(18)} = 7.6$, $p < 0.001$). Subsequent administration of HMWH increased this latency, i.e., had a significant reversal effect, that was significantly attenuated by the PI3Kγ inhibitor (Fig. 5*D*, right panel, $F_{(2,15)} = 6.9$, $p = 0.006$). Of note, in a separate experiment HMWH alone produced a similar increase in AP onset latency in neurons not exposed to PGE_2 (Fig. 5*D*, right panel). Additionally, ramp stimulation revealed HMWH-induced increase in AP threshold [by 4 ± 1 mV ($n = 6$), $t_{(5)} = 3.3$, $p = 0.02$]. The effect of HMWH was, however, no longer significant in the presence of the PI3Kγ inhibitor [0 ± 2 mV ($n = 6$), $t_{(5)} = 0.2$, $p = 0.8$]. There was a significant correlation between change in AP onset latency and change in AP threshold (Pearson's $r = 0.63$, $p = 0.038$, $n = 11$ pairs).

HMWH also increased the minimum slope of a current ramp required to induce an AP (Fig. 6*A*). While PGE_2 produced a reduction in the minimum slope (Fig. 6*B*, left panel, $t_{(7)} = 2.8$, $p = 0.03$), it was significantly increased following administration of HMWH, an effect that was not significant in the presence of PI3Kγ inhibitor, or without prior sensitization by PGE_2 (Fig. 6*B*, right panel, $F_{(2,16)} = 7.8$, $p = 0.004$).

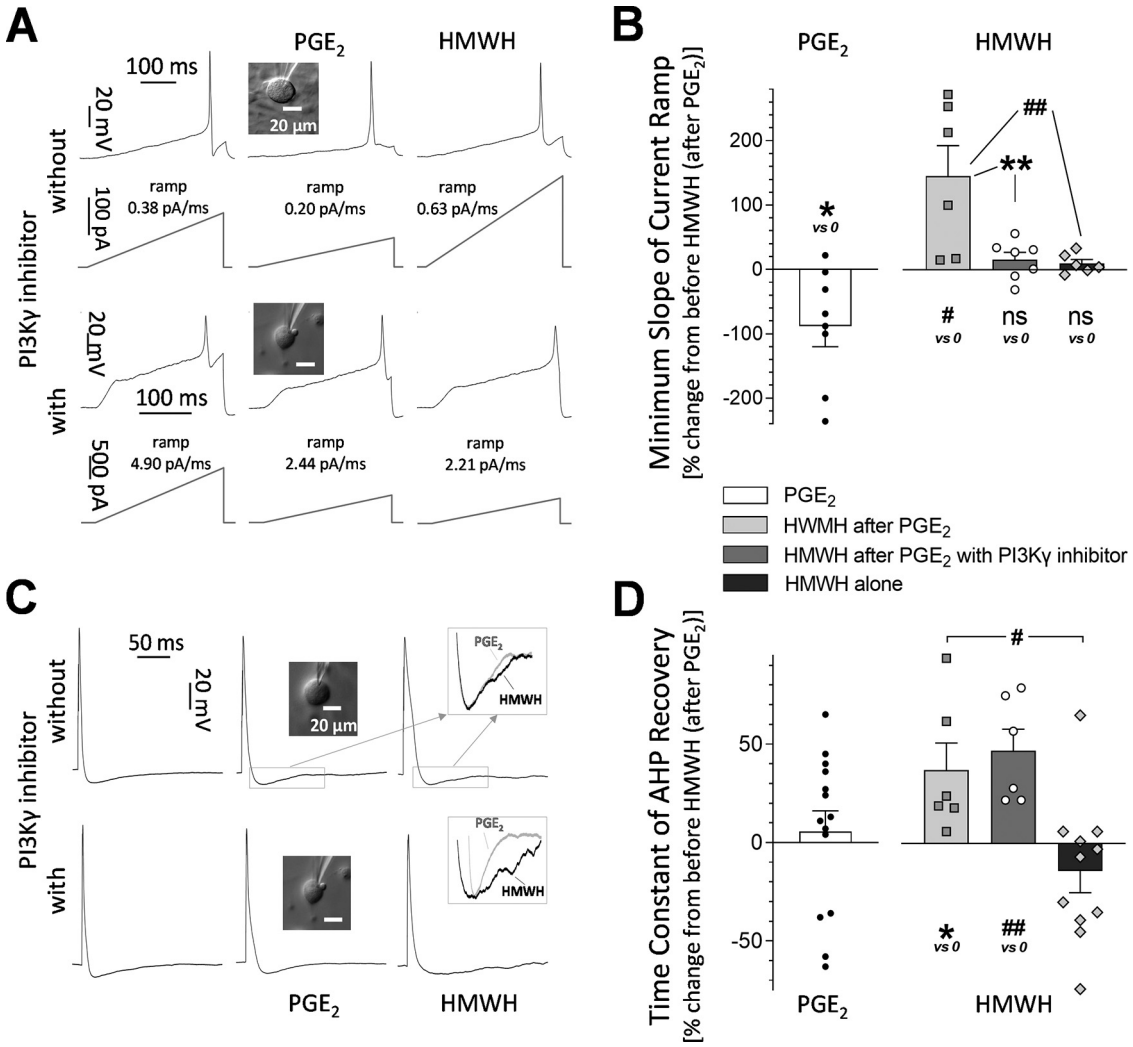

Figure 6. Sensitization-dependent and PI3Kγ-dependent effect of HMWH on biophysical parameters related to AP generation. ***A***, Example of HMWH-induced increase in the minimum slope of current ramp stimulation required to induce AP. Electrophysiological traces (upper) show APs generated in response to stimulation of a small DRG neuron (depicted in the inset image) with a current ramp (shown below AP recordings). Scale is the same for all traces. Note the HMWH-induced increase in the slope of the ramp (right traces) compared with its value after PGE_2 administration (middle trace). Such an increase was not observed in the presence of the selective PI3Kγ inhibitor, AS605240 (1 μM; second row of traces). ***B***, Effect of PGE_2 (left panel) and HMWH [alone and after PGE_2, with and without selective PI3Kγ inhibitor AS605240 (1 μM); right panel] on the minimum slope of current ramp stimulation required to induce an AP. PGE_2 produced significant reduction in the minimum ramp slope (one-sample two-tailed Student's *t* test for zero effect: $t_{(7)} = 2.76$, $^{*}p = 0.028$), while HMWH administered after PGE_2 produced statistically significant increase (i.e., reversal; one-sample two-tailed Student's *t* test for zero effect: $t_{(5)} = 3.05$, $^{\#}p = 0.028$). There was no statistically significant effect of HMWH on the minimum slope of the ramp when HMWH was applied alone (i.e., without prior sensitization by PGE_2) or after PGE_2, with a selective PI3Kγ inhibitor (one-sample two-tailed Student's *t* test for zero effect: $t_{(5)} = 1.53$, $p = 0.19$ for HMWH alone; $t_{(6)} = 1.36$, $p = 0.22$ with the inhibitor; ns = not statistically significant); the effects in both groups (with the PI3Kγ inhibitor and HMWH alone) were significantly smaller than the effect of HMWH administered after PGE_2 without PI3Kγ inhibitor (one-way ANOVA: $F_{(2,16)} = 7.75$, $p = 0.004$; Dunnett's *post hoc* test: $q_{(16)} = 3.42$, ** adjusted $p = 0.007$ with PI3Kγ inhibitor; $q_{(16)} = 3.45$, $^{\#\#}$ adjusted $p = 0.006$ for HMWH alone, when compared with HMWH after PGE_2), supporting the suggestion that the effect on latency depends on both activation of PI3Kγ and sensitization. Number of cells: eight for PGE_2, six for HMWH after PGE_2, seven for HMWH after PGE_2 with PI3Kγ inhibitor, and six for HMWH alone. ***C***, Example of HMWH-induced increase in the time constant of recovery of AHP phase of AP induced by a short current pulse at holding potential. Electrophysiological traces show APs generated in response to stimulation of a small DRG neuron, depicted in the inset image. Left trace is recorded before PGE_2, middle trace after PGE_2 (before HMWH), and trace to the right in the presence of HMWH, administered after the middle recording. Scale is the same among panels. Insets show AHP phase of the middle and right traces (indicated by light gray rectangles and arrows), overlayed, enlarged, and scaled to align minimums and baseline, to compare recovery rates. Note slower recovery of AHP phase of AP after application of HMWH (right traces) than after PGE_2 administration (middle trace), without a significant effect of the selective PI3Kγ inhibitor AS605240 (1 μM; second row of traces). ***D***, Effect of PGE_2 (left panel) and HMWH [alone and after PGE_2, with and without selective PI3Kγ inhibitor AS605240 (1 μM); right panel] on the time constant of recovery of AHP phase of AP. Legend for bar shading, symbols, and group order are the same as in ***A***. Effect of PGE_2 or HMWH, each alone, on the time constant of AHP recovery was not statistically significant (one-sample two-tailed Student's *t* test for zero effect: $t_{(13)} = 0.52$, $p = 0.61$ for PGE_2; $t_{(10)} = 1.28$, $p = 0.23$ for HMWH alone), while HMWH administered after PGE_2 produced a statistically significant increase (one-sample two-tailed Student's *t* test for zero effect: $t_{(5)} = 2.70$, $^{*}p = 0.043$). The selective PI3Kγ inhibitor did not have a statistically significant effect on HMWH-induced increase (one-way ANOVA: $F_{(2,20)} = 8.19$, $p = 0.003$; Dunnett's *post hoc* test: $q_{(20)} = 0.52$, adjusted $p = 0.82$ with PI3Kγ inhibitor; $q_{(20)} = 3.0$, $^{\#}$ adjusted $p = 0.013$ for HMWH alone, when compared with HMWH after PGE_2). The effect produced by HMWH after PGE_2 with PI3Kγ inhibitor was still statistically significant (one-sample two-tailed Student's *t* test for zero effect: $t_{(5)} = 4.36$, $^{\#\#}p = 0.007$), supporting the suggestion that the effect of HMWH on the recovery of AHP depends on sensitization but not activation of PI3Kγ. Number of cells: 14 for PGE_2, 6 for HMWH after PGE_2, 6 for HMWH after PGE_2 with PI3Kγ inhibitor, and 11 for HMWH alone. Of note, in ***B***, ***D***, the value before HMWH was used as a baseline to calculate the effect of HMWH, regardless of administration of PGE_2, whereas in the case of prior sensitization by PGE_2, "before HMWH" indicates the same value as "after PGE_2" and is used to calculate % change produced by PGE_2 as well (all in the same manner as in Fig. 5*D*).

Another mechanism that can contribute to AP frequency is recovery of the AP AHP. To examine whether HMWH affects the AHP recovery phase, a short stimulation (1- to 2-ms pulse), at baseline holding current, was used, allowing elimination of the interaction of AP AHP and stimulation (Fig. 6*C*). Magnitude of AHP (how deep below baseline) was not significantly changed either by PGE_2 or HMWH (data not shown). In contrast, time constant of recovery was significantly increased by HMWH applied after PGE_2, but not by PGE_2 or HMWH alone; this effect was not attenuated by PI3Kγ inhibitor (Fig. 6*D*, $t_{(13)} = 0.5$, $p = 0.6$ for PGE_2; $F_{(2,20)} = 8.2$, $p = 0.003$ for HMWH; $t_{(10)} = 1.3$, $p = 0.2$ for HMWH alone).

Discussion

Currently, little is known about the second messenger signaling pathway mediating HMWH anti-hyperalgesia or the electrophysiological properties of nociceptors impacted. HWMH signals through CD44, to activate PI3K (Fig. 7; Bourguignon et al., 2014). HMWH-induced anti-hyperalgesia is reversed by wortmannin and LY249002 (Bonet et al., 2020b) potent inhibitors of Class I, II, and III PI3K family members (Chaussade et al., 2007).

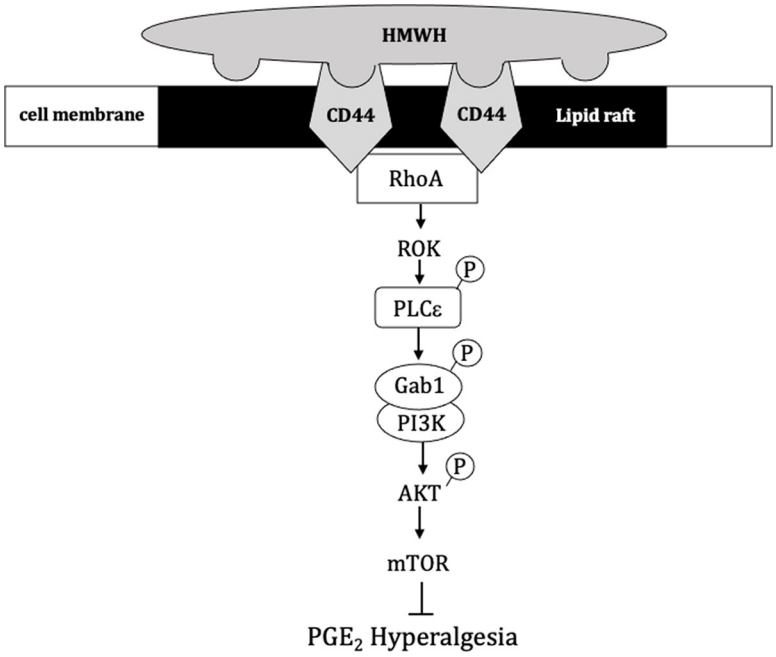

Figure 7. Schematic representation of signaling pathway mediating HMWH-induced anti-hyperalgesia. HMWH binds to CD44, its cognate receptor, to induce clustering in cell membrane lipid rafts and initiate signaling in downstream second messenger pathways. After HMWH binds to CD44, it can stimulate RhoA, which activates ROK to phosphorylate PLCε, increasing serine/threonine phosphorylation of the adaptor protein, Gab-1 and leading to activation of PI3Kγ/AKT/mTOR. CD44, cluster of differentiation 44 (hyaluronan receptor); RhoA, Rho family of GTPases; ROK, Rho-associated kinase; PLCε, phospholipase Cε; Gab1, scaffold protein; HMWH, high molecular weight hyaluronan; PI3K, phosphatidylinositol (PI) 3-kinase; AKT, protein kinase B; mTOR, mammalian target of rapamycin.

PI3K isoforms underly distinct, and sometimes opposing, functions (Vanhaesebroeck et al., 2010). Among the PI3K Class I isoforms present in DRG, PI3Kγ is expressed in small-diameter and medium-diameter neurons, which are predominantly C-fibers and Aδ-fibers (Pezet et al., 2008; Cunha et al., 2010; König et al., 2010; Leinders et al., 2014). Since it has been suggested that PI3Kγ/AKT signaling, rapidly activated by GPCRs, is involved in peripherally-induced antinociception by opioids (Cunha et al., 2010, 2012), we evaluated the hypothesis that PI3Kγ signals downstream of the HMWH receptor. Intrathecal administration of PI3Kγ antisense and a PI3Kγ-selective inhibitor (AS605240), administered adjacent to the nociceptor peripheral terminal, both markedly attenuates HMWH-induced anti-hyperalgesia, to a similar degree in both male and female rats. Of note, neither alone affects mechanical nociceptive threshold or PGE_2-induced hyperalgesia, excluding an independent role of PI3Kγ in setting nociceptive threshold or reversing hyperalgesia.

Since AKT and mTOR form a well-established PI3Kγ signaling pathway (Hawkins et al., 2006; Xu et al., 2020), we examined whether AKT was also involved in HMWH-induced anti-hyperalgesia. The selective inhibitor, AKT Inhibitor IV, attenuates HMWH-induced anti-hyperalgesia, while the injection of this inhibitor alone had no effect on nociceptive threshold. PI3K signaling can mediate hyperalgesia induced by nerve injury, incision, or inflammation (Pezet et al., 2008; Choi et al., 2010; Xu et al., 2014). And inhibition of PI3K attenuates mechanical allodynia (Pereira et al., 2011; Guan et al., 2015). Our results show an attenuation in HMWH-induced anti-hyperalgesia by inhibiting PI3Kγ/AKT signaling, in agreement with the previous demonstration that PI3K and AKT, in sensory neurons, can mediate the anti-hyperalgesic effects of MOR (Cunha et al., 2010, 2012).

AKT phosphorylates mTOR (Navé et al., 1999; Sekulić et al., 2000), which is expressed in sensory neurons, and contributes to pain transmission and modulation (Price et al., 2007; Geranton et al., 2009; Xu et al., 2011; Zhang et al., 2019). We found that rapamycin, administered at the peripheral terminal of the nociceptor, attenuates HMWH-induced anti-hyperalgesia. The mTOR signaling pathway integrates both intracellular and extracellular signals (Laplante and Sabatini, 2009, 2012). Activation of mTOR and its downstream effectors, in spinal cord, are implicated in cancer (Lucas and Lipman, 2002; Shih et al., 2012) and inflammatory (Liang et al., 2013) pain. Intrathecal administration of rapamycin produced anti-nociceptive effects in persistent inflammatory pain (Xu et al., 2011) and spared nerve injury (SNI)-induced mechanical allodynia (Geranton et al., 2009). However, western blot analysis of dorsal horn and dorsal roots, and immunostaining, showed no change in mTOR or the percentage of peripherin-labeled fibers expressing p-mTOR (Geranton et al., 2009). The mTOR protein is involved in multiprotein complexes, mTOR complex 1 (mTORC1) and mTOR complex 2 (mTORC2; Guertin and Sabatini, 2007). It has been shown that mTORC1 has a role in protein translation (Laplante and Sabatini, 2009). However, protein translation would seem an unlikely mechanism to mediate HMWH-induced anti-hyperalgesia given the rapid onset. In contrast to mTORC1, relatively little is known about mTORC2. While we have shown mTOR participating in the anti-hyperalgesic effect of HMWH, additional studies will be needed to clarify the functions of mTOR in antinociception. Taken together, our experiments provide evidence that HMWH-induced anti-hyperalgesia is dependent on PI3Kγ/AKT/mTOR signaling.

We have previously shown that HMWH can attenuate enhanced excitability of putative nociceptors sensitized by PGE_2,

in vitro, while not affecting rheobase or AP threshold in the absence of sensitization (Ferrari et al., 2018). HMWH partially reverses PGE_2-induced reduction in AP onset latency in response to current ramp stimulation (Ferrari et al., 2018), and attenuates tetrodotoxin (TTX)-resistant voltage-gated sodium current, important in PGE_2-induced hyperalgesia (England et al., 1996; Gold et al., 1998), in a PI3K-dependent manner (Bonet et al., 2020b). We explored the parameters of nociceptor excitability that were affected by HMWH, in sensitized nociceptors, in a way that reduces excitability, and examined whether identified changes were attenuated by a PI3Kγ inhibitor.

Stimulus intensity is encoded by number and frequency of APs (Bensmaïa et al., 2005; Muniak et al., 2007; Hao et al., 2015). PGE_2, which sensitizes ~60% of small-diameter DRG neurons (Gold et al., 1998; Khomula et al., 2021), putative C-type nociceptors (Woolf and Ma, 2007), increases these parameters (Gold et al., 1996; Momin and McNaughton, 2009). We found that HMWH can attenuate frequency and number of APs in neurons sensitized by PGE_2, effects that are PI3Kγ dependent.

In nociceptors, PGE_2 produces a prominent potentiating effect on sodium channels, and shift in voltage dependence of their activation to a more negative membrane potential, resulting in lower AP threshold potential, rheobase and AP onset latency, in response to current ramp stimulation (Ferrari et al., 2018). However, reduction in rheobase and AP threshold was not affected by HMWH. Also, absence of a significant effect of HMWH on AP threshold potential supports the suggestion that previously reported PI3K-dependent HMWH-induced inhibition of TTX-resistant voltage-gated sodium current (Bonet et al., 2020a) was not because of shift in voltage dependence of their activation. Lack of effect of the PI3Kγ inhibitor on the HMWH-induced reduction in AP peak potential correlates with the above-mentioned inhibition of sodium current and indirectly indicates it was not dependent on PI3Kγ. HMWH-induced inhibition of sodium current may, however, still impact the generation of consequent APs, thus influencing firing frequency.

HMWH increased the latency to AP onset during ramp current stimulation, another measure of excitability. This effect was PI3Kγ dependent. HMWH produced a similar increase in AP onset latency in neurons not exposed to PGE_2, suggesting a sensitization-independent effect on nociceptor excitability. As HMWH increased the magnitude of current required for AP generation (latency to AP onset multiplied by slope of current ramp), this effect may contribute to the attenuation of neuronal activity, including the observed decrease in frequency and number of APs. Of note, while HMWH did not affect AP threshold potential during immediate onset of stimulus (in step current protocol, used to measure rheobase), gradual depolarization in ramp protocol revealed PI3Kγ-dependent increase in AP threshold potential, which significantly correlated with the increase in AP onset latency. This finding supports the suggestion that HMWH-induced change in AP threshold contributes to the effect of HMWH on nociceptor excitability and compatible with HMWH-induced modulation of TTX-resistant voltage-gated sodium channels, which are activated and inactivated at higher membrane potentials, along with HMWH-induced potentiation of a "breaking" mechanism (e.g., increase in subthreshold potassium conductance or facilitation of inactivation of sodium channels).

We also found that in sensitized nociceptors HMWH affected the minimum slope of a current ramp (i.e., rate of stimulus onset required to induce an AP) recently reported as an important characteristic of excitability of sensory neurons, a parameter that is dependent on low-threshold activated D-type potassium current (Sun, 2021). While the minimum rate of stimulus onset required to induce an AP was significantly reduced by PGE_2 (thus contributing to sensitization), the subsequent administration of HMWH markedly increased this parameter thus reversing PGE_2-induced changes in a parameter of excitability; likely contributing to HMWH-induced anti-hyperalgesia. The effect of HMWH on this parameter was markedly attenuated in the presence of the PI3Kγ inhibitor and was not significant without prior sensitization. Our findings support the suggestion that HMWH-induced anti-hyperalgesia involves PI3Kγ-dependent signaling mechanisms, which are enabled by nociceptor sensitization. Furthermore, taking into account that both HMWH-induced reduction in AP firing rate and HMWH-induced increase in the minimum stimulus onset rate are PI3Kγ-dependent, we may assume the existence of shared underlying HMWH-regulated PI3Kγ-dependent ionic mechanisms, for instance potentiation of low-threshold potassium channels.

Duration of the AHP phase of an AP can influence firing frequency (Deister et al., 2009; Vandael et al., 2010; Jaffe and Brenner, 2018). We found that HMWH slowed AHP recovery rate, but only when administered after PGE_2. This effect of HMWH was not, however, altered by a PI3Kγ inhibitor, supporting the suggestion that it is mediated by a PI3Kγ-independent branch of HMWH signaling pathways. Of note, PGE_2 by itself, as well as HMWH alone, did not affect this parameter. Thus, the observed effect was produced by HMWH, specifically in sensitized nociceptors.

Our *in vitro* findings support the suggestion that HMWH-induced alterations in electrophysiological mechanisms of AP generation in nociceptors play a role in HMWH-induced anti-hyperalgesia. HMWH attenuated PGE_2-induced changes in some parameters of nociceptor excitability and produced additional changes in parameters unrelated to effects of PGE_2. Some, but not all HMWH-induced changes were dependent on PI3Kγ and/or prior sensitization. Ongoing experiments are exploring the PI3Kγ-independent mechanisms mediating HMWH anti-hyperalgesia.

In conclusion, our finds that a PI3Kγ-dependent signaling pathway is involved in HWMH-induced anti-hyperalgesia and nociceptor sensitization (Fig. 7) opens a novel line of research into molecular targets for the treatment of pain produced by nociceptor sensitization.

References

Alessandri-Haber N, Yeh JJ, Boyd AE, Parada CA, Chen X, Reichling DB, Levine JD (2003) Hypotonicity induces TRPV4-mediated nociception in rat. Neuron 39:497–511.

Ali K, Camps M, Pearce WP, Ji H, Rückle T, Kuehn N, Pasquali C, Chabert C, Rommel C, Vanhaesebroeck B (2008) Isoform-specific functions of phosphoinositide 3-kinases: p110 delta but not p110 gamma promotes optimal allergic responses in vivo. J Immunol 180:2538–2544.

Altman RD, Moskowitz R (1998) Intraarticular sodium hyaluronate (Hyalgan) in the treatment of patients with osteoarthritis of the knee: a randomized clinical trial. Hyalgan study group. J Rheumatol 25:2203–2212.

Alvarez P, Green PG, Levine JD (2014) Role for monocyte chemoattractant protein-1 in the induction of chronic muscle pain in the rat. Pain 155:1161–1167.

Araldi D, Ferrari LF, Levine JD (2017) Hyperalgesic priming (type II) induced by repeated opioid exposure: maintenance mechanisms. Pain 158:1204–1216.

Araldi D, Bogen O, Green PG, Levine JD (2019) Role of nociceptor Toll-like receptor 4 (TLR4) in opioid-induced hyperalgesia and hyperalgesic priming. J Neurosci 39:6414–6424.

Bensmaïa SJ, Leung YY, Hsiao SS, Johnson KO (2005) Vibratory adaptation of cutaneous mechanoreceptive afferents. J Neurophysiol 94:3023–3036.

Bogen O, Alessandri-Haber N, Chu C, Gear RW, Levine JD (2012) Generation of a pain memory in the primary afferent nociceptor triggered by PKCε activation of CPEB. J Neurosci 32:2018–2026.

Bonet IJM, Green PG, Levine JD (2020a) Sexual dimorphism in the nociceptive effects of hyaluronan. Pain 162:1116–1125.

Bonet IJM, Araldi D, Khomula EV, Bogen O, Green PG, Levine JD (2020b) Mechanisms mediating high-molecular-weight hyaluronan-induced antihyperalgesia. J Neurosci 40:6477–6488.

Borle AB, Snowdowne KW (1982) Measurement of intracellular free calcium in monkey kidney cells with aequorin. Science 217:252–254.

Bourguignon LY, Shiina M, Li JJ (2014) Hyaluronan-CD44 interaction promotes oncogenic signaling, microRNA functions, chemoresistance, and radiation resistance in cancer stem cells leading to tumor progression. Adv Cancer Res 123:255–275.

Burch RM, Axelrod J (1987) Dissociation of bradykinin-induced prostaglandin formation from phosphatidylinositol turnover in Swiss 3T3 fibroblasts: evidence for G protein regulation of phospholipase A2. Proc Natl Acad Sci USA 84:6374–6378.

Caires R, Luis E, Taberner FJ, Fernandez-Ballester G, Ferrer-Montiel A, Balazs EA, Gomis A, Belmonte C, de la Peña E (2015) Hyaluronan modulates TRPV1 channel opening, reducing peripheral nociceptor activity and pain. Nat Commun 6:8095.

Chaussade C, Rewcastle GW, Kendall JD, Denny WA, Cho K, Grønning LM, Chong ML, Anagnostou SH, Jackson SP, Daniele N, Shepherd PR (2007) Evidence for functional redundancy of class IA PI3K isoforms in insulin signalling. Biochem J 404:449–458.

Choi JI, Svensson CI, Koehrn FJ, Bhuskute A, Sorkin LS (2010) Peripheral inflammation induces tumor necrosis factor dependent AMPA receptor trafficking and Akt phosphorylation in spinal cord in addition to pain behavior. Pain 149:243–253.

Cohen LB, Keynes RD, Hille B (1968) Light scattering and birefringence changes during nerve activity. Nature 218:438–441.

Cohen MM, Altman RD, Hollstrom R, Hollstrom C, Sun C, Gipson B (2008) Safety and efficacy of intra-articular sodium hyaluronate (Hyalgan) in a randomized, double-blind study for osteoarthritis of the ankle. Foot Ankle Int 29:657–663.

Cuff CA, Kothapalli D, Azonobi I, Chun S, Zhang Y, Belkin R, Yeh C, Secreto A, Assoian RK, Rader DJ, Puré E (2001) The adhesion receptor CD44 promotes atherosclerosis by mediating inflammatory cell recruitment and vascular cell activation. J Clin Invest 108: 1031–1040.

Cunha TM, Roman-Campos D, Lotufo CM, Duarte HL, Souza GR, Verri WA Jr, Funez MI, Dias QM, Schivo IR, Domingues AC, Sachs D, Chiavegatto S, Teixeira MM, Hothersall JS, Cruz JS, Cunha FQ, Ferreira SH (2010) Morphine peripheral analgesia depends on activation of the PI3Kgamma/AKT/nNOS/NO/KATP signaling pathway. Proc Natl Acad Sci USA 107:4442–4447.

Cunha TM, Souza GR, Domingues AC, Carreira EU, Lotufo CM, Funez MI, Verri WA Jr, Cunha FQ, Ferreira SH (2012) Stimulation of peripheral kappa opioid receptors inhibits inflammatory hyperalgesia via activation of the PI3Kγ/AKT/nNOS/NO signaling pathway. Mol Pain 8:10.

de la Peña E, Gomis A, Ferrer-Montiel A, Belmonte C (2016) TRPV1 channel modulation by hyaluronan reduces pain. Channels (Austin) 10:81–82.

Deister CA, Chan CS, Surmeier DJ, Wilson CJ (2009) Calcium-activated SK channels influence voltage-gated ion channels to determine the precision of firing in globus pallidus neurons. J Neurosci 29:8452–8461.

Dougados M, Nguyen M, Listrat V, Amor B (1993) High molecular weight sodium hyaluronate (hyalectin) in osteoarthritis of the knee: a 1 year placebo-controlled trial. Osteoarthritis Cartilage 1:97–103.

Duzhyy DE, Viatchenko-Karpinski VY, Khomula EV, Voitenko NV, Belan PV (2015) Upregulation of T-type Ca2+ channels in long-term diabetes determines increased excitability of a specific type of capsaicin-insensitive DRG neurons. Mol Pain 11:29.

Eickholt BJ, Ahmed AI, Davies M, Papakonstanti EA, Pearce W, Starkey ML, Bilancio A, Need AC, Smith AJ, Hall SM, Hamers FP, Giese KP, Bradbury EJ, Vanhaesebroeck B (2007) Control of axonal growth and regeneration of sensory neurons by the p110delta PI 3-kinase. PLoS One 2:e869.

Engelman JA, Luo J, Cantley LC (2006) The evolution of phosphatidylinositol 3-kinases as regulators of growth and metabolism. Nat Rev Genet 7:606–619.

England S, Bevan S, Docherty RJ (1996) PGE2 modulates the tetrodotoxin-resistant sodium current in neonatal rat dorsal root ganglion neurones via the cyclic AMP-protein kinase A cascade. J Physiol 495 (Pt 2):429–440.

Ferrari LF, Khomula EV, Araldi D, Levine JD (2016a) Marked sexual dimorphism in the role of the ryanodine receptor in a model of pain chronification in the rat. Sci Rep 6:31221.

Ferrari LF, Araldi D, Bogen O, Levine JD (2016b) Extracellular matrix hyaluronan signals via its CD44 receptor in the increased responsiveness to mechanical stimulation. Neuroscience 324:390–398.

Ferrari LF, Khomula EV, Araldi D, Levine JD (2018) CD44 signaling mediates high molecular weight hyaluronan-induced antihyperalgesia. J Neurosci 38:308–321.

Franke TF, Hornik CP, Segev L, Shostak GA, Sugimoto C (2003) PI3K/Akt and apoptosis: size matters. Oncogene 22:8983–8998.

Furuta J, Ariyoshi W, Okinaga T, Takeuchi J, Mitsugi S, Tominaga K, Nishihara T (2017) High molecular weight hyaluronic acid regulates MMP13 expression in chondrocytes via DUSP10/MKP5. J Orthop Res 35:331–339.

Geranton SM, Jimenez-Diaz L, Torsney C, Tochiki KK, Stuart SA, Leith JL, Lumb BM, Hunt SP (2009) A rapamycin-sensitive signaling pathway is essential for the full expression of persistent pain states. J Neurosci 29:15017–15027.

Gold MS, Dastmalchi S, Levine JD (1996) Co-expression of nociceptor properties in dorsal root ganglion neurons from the adult rat in vitro. Neuroscience 71:265–275.

Gold MS, Levine JD, Correa AM (1998) Modulation of TTX-R INa by PKC and PKA and their role in PGE2-induced sensitization of rat sensory neurons in vitro. J Neurosci 18:10345–10355.

Gomis A, Miralles A, Schmidt RF, Belmonte C (2007) Nociceptive nerve activity in an experimental model of knee joint osteoarthritis of the guinea pig: effect of intra-articular hyaluronan application. Pain 130:126–136.

Gruber JV, Holtz R, Riemer J (2021) Hyaluronic acid (HA) stimulates the in vitro expression of CD44 proteins but not HAS1 proteins in normal human epidermal keratinocytes (NHEKs) and is HA molecular weight dependent. J Cosmet Dermatol. Advance online publication. Retrieved Apr 28, 2021. doi: 10.1111/jocd.14188.

Guan XH, Fu QC, Shi D, Bu HL, Song ZP, Xiong BR, Shu B, Xiang HB, Xu B, Manyande A, Cao F, Tian YK (2015) Activation of spinal chemokine receptor CXCR3 mediates bone cancer pain through an Akt-ERK crosstalk pathway in rats. Exp Neurol 263:39–49.

Guertin DA, Sabatini DM (2007) Defining the role of mTOR in cancer. Cancer Cell 12:9–22.

Hao J, Bonnet C, Amsalem M, Ruel J, Delmas P (2015) Transduction and encoding sensory information by skin mechanoreceptors. Pflugers Arch 467:109–119.

Harper AA, Lawson SN (1985) Conduction velocity is related to morphological cell type in rat dorsal root ganglion neurones. J Physiol 359:31–46.

Hawkins PT, Anderson KE, Davidson K, Stephens LR (2006) Signalling through class I PI3Ks in mammalian cells. Biochem Soc Trans 34:647–662.

Huang TL, Chang CC, Lee CH, Chen SC, Lai CH, Tsai CL (2011) Intra-articular injections of sodium hyaluronate (Hyalgan(R)) in osteoarthritis of the knee. a randomized, controlled, double-blind, multicenter trial in the Asian population. BMC Musculoskelet Disord 12:221.

Jaffe DB, Brenner R (2018) A computational model for how the fast afterhyperpolarization paradoxically increases gain in regularly firing neurons. J Neurophysiol 119:1506–1520.

Jin JR, Gogvadze E, Xavier AR, Bohnacker T, Voelzmann J, Wymann MP (2020) PI3Kγ regulatory protein p84 determines mast cell sensitivity to Ras inhibition-moving towards cell specific PI3K targeting? Front Immunol 11:585070.

Kataoka Y, Ariyoshi W, Okinaga T, Kaneuji T, Mitsugi S, Takahashi T, Nishihara T (2013) Mechanisms involved in suppression of ADAMTS4 expression in synoviocytes by high molecular weight hyaluronic acid. Biochem Biophys Res Commun 432:580–585.

Khomula EV, Araldi D, Levine JD (2019) In vitro nociceptor neuroplasticity associated with in vivo opioid-induced hyperalgesia. J Neurosci 39:7061–7073.

Khomula EV, Araldi D, Bonet IJM, Levine JD (2021) Opioid-induced hyperalgesic priming in single nociceptors. J Neurosci 41:31–46.

König C, Gavrilova-Ruch O, von Banchet GS, Bauer R, Grün M, Hirsch E, Rubio I, Schulz S, Heinemann SH, Schaible HG, Wetzker R (2010) Modulation of mu opioid receptor desensitization in peripheral sensory neurons by phosphoinositide 3-kinase gamma. Neuroscience 169:449–454.

Landowne D (1993) Measuring nerve excitation with polarized light. Jpn J Physiol 43:S7–S11.

Laplante M, Sabatini DM (2009) mTOR signaling at a glance. J Cell Sci 122:3589–3594.

Laplante M, Sabatini DM (2012) mTOR signaling in growth control and disease. Cell 149:274–293.

Leinders M, Koehrn FJ, Bartok B, Boyle DL, Shubayev V, Kalcheva I, Yu NK, Park J, Kaang BK, Hefferan MP, Firestein GS, Sorkin LS (2014) Differential distribution of PI3K isoforms in spinal cord and dorsal root ganglia: potential roles in acute inflammatory pain. Pain 155:1150–1160.

Liang L, Tao B, Fan L, Yaster M, Zhang Y, Tao YX (2013) mTOR and its downstream pathway are activated in the dorsal root ganglion and spinal cord after peripheral inflammation, but not after nerve injury. Brain Res 1513:17–25.

Lucas LK, Lipman AG (2002) Recent advances in pharmacotherapy for cancer pain management. Cancer Pract 10 [Suppl 1]:S14–S20.

Mestre C, Pélissier T, Fialip J, Wilcox G, Eschalier A (1994) A method to perform direct transcutaneous intrathecal injection in rats. J Pharmacol Toxicol Methods 32:197–200.

Mizrahy S, Raz SR, Hasgaard M, Liu H, Soffer-Tsur N, Cohen K, Dvash R, Landsman-Milo D, Bremer MG, Moghimi SM, Peer D (2011) Hyaluronan-coated nanoparticles: the influence of the molecular weight on CD44-hyaluronan interactions and on the immune response. J Control Release 156:231–238.

Momin A, McNaughton PA (2009) Regulation of firing frequency in nociceptive neurons by pro-inflammatory mediators. Exp Brain Res 196:45–52.

Morello F, Perino A, Hirsch E (2009) Phosphoinositide 3-kinase signalling in the vascular system. Cardiovasc Res 82:261–271.

Muniak MA, Ray S, Hsiao SS, Dammann JF, Bensmaïa SJ (2007) The neural coding of stimulus intensity: linking the population response of mechanoreceptive afferents with psychophysical behavior. J Neurosci 27:11687–11699.

Navé BT, Ouwens M, Withers DJ, Alessi DR, Shepherd PR (1999) Mammalian target of rapamycin is a direct target for protein kinase B: identification of a convergence point for opposing effects of insulin and amino-acid deficiency on protein translation. Biochem J 344 [Pt 2]:427–431.

Oliveira-Fusaro MCG, Zanoni CIS, Dos Santos GG, Manzo LP, Araldi D, Bonet IJM, Tambeli CH, Dias EV, Parada CA (2017) Antihyperalgesic effect of CB1 receptor activation involves the modulation of P2X3 receptor in the primary afferent neuron. Eur J Pharmacol 798:113–121.

Parada CA, Yeh JJ, Reichling DB, Levine JD (2003) Transient attenuation of protein kinase Cε can terminate a chronic hyperalgesic state in the rat. Neuroscience 120:219–226.

Pereira PJS, Lazarotto LF, Leal PC, Lopes TG, Morrone FB, Campos MM (2011) Inhibition of phosphatidylinositol-3 kinase γ reduces pruriceptive, inflammatory, and nociceptive responses induced by trypsin in mice. Pain 152:2861–2869.

Petruska JC, Napaporn J, Johnson RD, Gu JG, Cooper BY (2000) Subclassified acutely dissociated cells of rat DRG: histochemistry and patterns of capsaicin-, proton-, and ATP-activated currents. J Neurophysiol 84:2365–2379.

Petruska JC, Napaporn J, Johnson RD, Cooper BY (2002) Chemical responsiveness and histochemical phenotype of electrophysiologically classified cells of the adult rat dorsal root ganglion. Neuroscience 115:15–30.

Pezet S, Marchand F, D'Mello R, Grist J, Clark AK, Malcangio M, Dickenson AH, Williams RJ, McMahon SB (2008) Phosphatidylinositol 3-kinase is a key mediator of central sensitization in painful inflammatory conditions. J Neurosci 28:4261–4270.

Price TJ, Rashid MH, Millecamps M, Sanoja R, Entrena JM, Cervero F (2007) Decreased nociceptive sensitization in mice lacking the fragile X mental retardation protein: role of mGluR1/5 and mTOR. J Neurosci 27:13958–13967.

Pritchard RA, Falk L, Larsson M, Leinders M, Sorkin LS (2016) Different phosphoinositide 3-kinase isoforms mediate carrageenan nociception and inflammation. Pain 157:137–146.

Quanhong Z, Ying X, Moxi C, Tao X, Jing W, Xin Z, Li W, Derong C, Xiaoli Z, Wei J (2012) Intrathecal PLC(β3) oligodeoxynucleotides antisense potentiates acute morphine efficacy and attenuates chronic morphine tolerance. Brain Res 1472:38–44.

Randall LO, Selitto JJ (1957) A method for measurement of analgesic activity on inflamed tissue. Arch Int Pharmacodyn Ther 111:409–419.

Rommel C, Camps M, Ji H (2007) PI3K delta and PI3K gamma: partners in crime in inflammation in rheumatoid arthritis and beyond? Nat Rev Immunol 7:191–201.

Rückle T, Schwarz MK, Rommel C (2006) PI3Kgamma inhibition: towards an 'aspirin of the 21st century'? Nat Rev Drug Discov 5:903–918.

Sekulić A, Hudson CC, Homme JL, Yin P, Otterness DM, Karnitz LM, Abraham RT (2000) A direct linkage between the phosphoinositide 3-kinase-AKT signaling pathway and the mammalian target of rapamycin in mitogen-stimulated and transformed cells. Cancer Res 60:3504–3513.

Shaw RJ, Cantley LC (2006) Ras, PI(3)K and mTOR signalling controls tumour cell growth. Nature 441:424–430.

Shih MH, Kao SC, Wang W, Yaster M, Tao YX (2012) Spinal cord NMDA receptor-mediated activation of mammalian target of rapamycin is required for the development and maintenance of bone cancer-induced pain hypersensitivities in rats. J Pain 13:338–349.

Song MJ, Wang YQ, Wu GC (2009) Additive anti-hyperalgesia of electroacupuncture and intrathecal antisense oligodeoxynucleotide to interleukin-1 receptor type I on carrageenan-induced inflammatory pain in rats. Brain Res Bull 78:335–341.

Su L, Wang C, Yu YH, Ren YY, Xie KL, Wang GL (2011) Role of TRPM8 in dorsal root ganglion in nerve injury-induced chronic pain. BMC Neurosci 12:120.

Sun H (2021) Different Sensitivity of action potential generation to the rate of depolarization in vagal afferent A-fiber versus C-fiber neurons. J Neurophysiol 125:2000–2012.

Sun JL, Xiao C, Lu B, Zhang J, Yuan XZ, Chen W, Yu LN, Zhang FJ, Chen G, Yan M (2013) CX3CL1/CX3CR1 regulates nerve injury-induced pain hypersensitivity through the ERK5 signaling pathway. J Neurosci Res 91:545–553.

Taiwo YO, Levine JD (1989) Prostaglandin effects after elimination of indirect hyperalgesic mechanisms in the skin of the rat. Brain Res 492:397–399.

Taiwo YO, Coderre TJ, Levine JD (1989) The contribution of training to sensitivity in the nociceptive paw-withdrawal test. Brain Res 487:148–151.

Tavianatou AG, Caon I, Franchi M, Piperigkou Z, Galesso D, Karamanos NK (2019) Hyaluronan: molecular size-dependent signaling and biological functions in inflammation and cancer. FEBS J 286:2883–2908.

Toole BP (2009) Hyaluronan-CD44 interactions in cancer: paradoxes and possibilities. Clin Cancer Res 15:7462–7468.

Triantaffilidou K, Venetis G, Bika O (2013) Efficacy of hyaluronic acid injections in patients with osteoarthritis of the temporomandibular joint. A comparative study. J Craniofac Surg 24:2006–2009.

Vandael DH, Marcantoni A, Mahapatra S, Caro A, Ruth P, Zuccotti A, Knipper M, Carbone E (2010) Ca(v)1.3 and BK channels for timing and regulating cell firing. Mol Neurobiol 42:185–198.

Vanhaesebroeck B, Guillermet-Guibert J, Graupera M, Bilanges B (2010) The emerging mechanisms of isoform-specific PI3K signalling. Nat Rev Mol Cell Biol 11:329–341.

Viatchenko-Karpinski V, Gu JG (2016) Mechanical sensitivity and electrophysiological properties of acutely dissociated dorsal root ganglion neurons of rats. Neurosci Lett 634:70–75.

Vigetti D, Viola M, Karousou E, De Luca G, Passi A (2014a) Metabolic control of hyaluronan synthases. Matrix Biol 35:8–13.

Vigetti D, Karousou E, Viola M, Deleonibus S, De Luca G, Passi A (2014b) Hyaluronan: biosynthesis and signaling. Biochim Biophys Acta 1840:2452–2459.

Woolf CJ, Ma Q (2007) Nociceptors–noxious stimulus detectors. Neuron 55:353–364.

Wu PT, Kuo LC, Su FC, Chen SY, Hsu TI, Li CY, Tsai KJ, Jou IM (2017) High-molecular-weight hyaluronic acid attenuated matrix metalloproteinase-1 and -3 expression via CD44 in tendinopathy. Sci Rep 7:40840.

Wullschleger S, Loewith R, Hall MN (2006) TOR signaling in growth and metabolism. Cell 124:471–484.

Xu B, Guan XH, Yu JX, Lv J, Zhang HX, Fu QC, Xiang HB, Bu HL, Shi D, Shu B, Qin LS, Manyande A, Tian YK (2014) Activation of spinal phosphatidylinositol 3-kinase/protein kinase B mediates pain behavior induced by plantar incision in mice. Exp Neurol 255:71–82.

Xu F, Na L, Li Y, Chen L (2020) Roles of the PI3K/AKT/mTOR signalling pathways in neurodegenerative diseases and tumours. Cell Biosci 10:54.

Xu Q, Fitzsimmons B, Steinauer J, O'Neill A, Newton AC, Hua XY, Yaksh TL (2011) Spinal phosphinositide 3-kinase-Akt-mammalian target of rapamycin signaling cascades in inflammation-induced hyperalgesia. J Neurosci 31:2113–2124.

Zhang X, Jiang N, Li J, Zhang D, Lv X (2019) Rapamycin alleviates proinflammatory cytokines and nociceptive behavior induced by chemotherapeutic paclitaxel. Neurol Res 41:52–59.